ORIGINAL RESEARCH PAPER

Electronic Behavior of Doped Graphene Nanoribbon Device: NEGF+DFT

Sadegh Afshari [1]*, Jaber Jahanbin Sardroodi [2], Hakimeh Mohammadpour [3]

[1] School of Chemistry, Damghan University, Damghan, Iran
[2] Molecular Simulation Lab., Azarbaijan Shahid Madani University, Tabriz, Iran
[3] Department of Physics, Azarbaijan Shahid Madani University, Tabriz, Iran

Received: 2017-07-10 Accepted: 2017-10-19 Published: 2017-12-20

ABSTRACT
Quantum transport properties of pure and functioned infinite lead-connection region-lead system based on the zigzag graphene nanoribbon (2-zGNR) have been investigated. In this work the effect of the doping functionalization on the quantum transport of the 2-zGNR has been computationally studied. Also, the effect of the imposed gate voltages (-3.0, 0.0 and +3.0 V) and bias voltages 0.0 to 2.0 V have been studied. The results were presented as the current versus the bias voltage (I-V_b) curves with unique properties for per studied systems, showing one or two negative differential resistances (NDR). The NDR region was discussed and interpreted in the terms of the transmission spectrum and its integral inside of the corresponding bias window. Also, the partial atomic charge distribution in the center part of the system's scattering region containing carbon atoms at the left and right sides of substituted atoms which are connected to substituted atoms has been investigated for different bias voltages.

Keywords: *graphene nanoribbon; partial atomic charge; NEGF; NDR; doping*

How to cite this article
Afshari S, Jahanbin Sardroodi J, Mohammadpour H. Electronic Behavior of Doped Graphene Nanoribbon Device: NEGF+DFT. J. Nanoanalysis., 2017; 4(4): 272-279. DOI: 10.22034/jna.2017.539940

INTRODUCTION

The potential application of new molecular-based materials in nano-electronics have attracted attention from both of the research and applied science communities. Identification and understanding of interesting properties, such as molecular rectifying, [1, 2] negative differential resistance (NDR)[3, 4] and switch behaviors, [5, 6] etc., have provided opportunity for controlling of the electron transport phenomena of molecular structures. Several ways of modulating the transport properties of different molecular devices, such as group effects, [7, 8] doping effects, [9, 10] length effects, [11, 12] strain effects, [13] edge effects[14] and thermal effects, [15, 16] etc., have been in the focus of considerations. Among these, molecular junctions have been attracted significant due to their potential application in nanoelectronics switch tunable properties of the single molecule level attention in the past decade. Many interesting physical properties, such as conducting, ratifying, resisting, switching and amplifying have been demonstrated in molecular junctions. The NDR effect, which stands for

* Corresponding Author Email: s.afshari@du.ac.ir

decreasing in current by increasing the bias voltage, has an important role in electronics. Transport properties including NDR have been discussed in various molecular junctions,[17] between carbon nanotubes[18-23] and other metal electrodes such as gold. [24-28] Out of many molecular structures, Graphene has attracted vast attention specially from nanoelectronics community for its novel electronic properties, [29] planer structure, optical transparency and conductivity [30-36], etc. In order to open an energy gap in the graphene some modifications, such as cutting it to the graphene nanoribbon (GNR) stripes, can be applied to form unique structures possessing various electronic properties. Many feasible approaches to change the properties of GNRs such as chemical functionalization, [37, 38] doping, [39-41] defect, [42, 43] hybridized connection, [44-46] mechanical stretch, [47, 48] adsorption, [49, 50] and layer stacking [51-53] have been proposed. In most of the recent studies, the chemical modification is an effective way in device design. The fluorinated GNRs, BN sheets, BN nanotubes, etc., have been reported.

In this work we have investigated computationally a GNR-junction with different chemical modifications to the junction. Our model consists of two contacts and a scattering region through which the current is carried between the contacts held at different bias voltages. The system is an infinite zigzag GNR with a chemically modified regional at the midway that acts as scattering region. The resultant current-voltage curves indicate NDR phenomena in the case of adjusting atoms, different from carbon, at the junction. This provides a great promise in the field of nanoelectronics. We have attributed the origin of the NDR in such that junctions with weakly coupled contacts, to the narrow density of state (DOS) features of the junction and have justified it by the calculated DOS diagrams.

MODEL AND COMPUTATIONAL METHOD

The systems under investigation were infinite lead-connection region-lead systems based on zigzag graphene nanoribbon. The infinite ribbons are composed of a benzene ring in the width direction (i.e., 2-zGNR) and are divided into the left- and right- leads held at different voltages. The connection region between the two leads is chemically modified by different compounds manifesting the scattering region, figure 1. The doping atoms we have employed are Silicon and Germanium (the green atoms) and up and down the edges of the nanoribbon are hydrogen-passivated. The calculations were carried out with OpenMX computer code.[54] DFT within the generalized gradient approximation (GGA)[55] for the exchange-correlation energy was adopted. Norm-conserving Kleinman–Bylander pseudopotentials[56] were employed, and the wave functions were expanded by a linear combination of multiple pseudo-atomic orbitals (LCPAO)[57, 58].

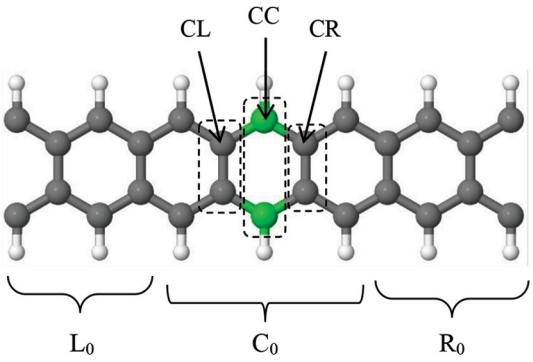

Fig. 1: Schematic illustrations of 2-ZGNR.Green atoms are presented as substituted Carbon atoms by Silicon or Germanium. Hydrogen and Carbon atoms are colored in white and grey, respectively.

RESULTS AND DISCUSSION

Transport properties

First, the transport properties of the pure and doped (Silicon and Germanium) graphene nanoribbons have been probed. The transmission function, T(E) is the most important physical quantity in NEGF-DFT calculations for the electronic transport. This quantity is determined by the scattering rate of the (doped) channel region located between the two leads. For clarifying, the Fermi level has been set to E_F=0. For the system at equilibrium, the conductance G is evaluated by the transmission coefficients T(E) at the Fermi energy E_F of the system $G=G_0T(E_F)$, where $G_0=2e^2/h$ is the fundamental quantum conductance unit. The calculated T(E) is shown in figure 2. It is strongly energy dependent with local minima and maxima up to 2 (including spin of electrons). Besides the differences between the diagrams of different studied systems, the locations of the maxima and minima in energy axes of the transmission function are almost the same for the three systems. To probe this behavior of T (E), the diagrams of the transmission probability and the density of states (DOS) at the channel region, versus energy depicted have been plotted in figure 3 (a-c) for the three systems. The qualitative (however, not of the same

dimensions) overlap between the two parameters reveals the evident dependence of the transmission probability of the electronic density of the channel.

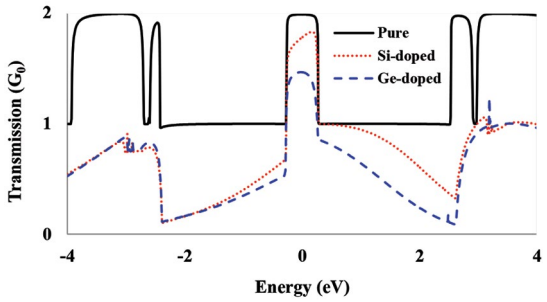

Fig. 2: Transmission spectrums for the three studied systems.

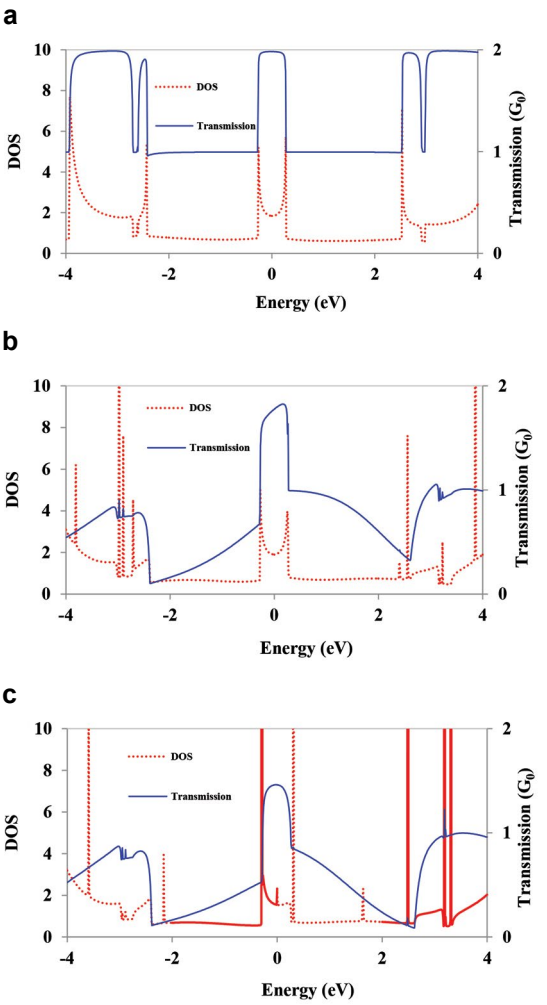

Fig. 3: Transmission and DOS spectrums for a) pure, b) Si-doped, and c) Ge-doped 2-zGNR's.

characteristics

The structural symmetric molecular junction will result in a current-voltage (I-V) curve that is symmetric with respect to the Voltage sign change, while an asymmetric junction results in an asymmetric I-V_b curve. So, regarding the studied structures with high symmetry in the electronic transport direction, we have obtained symmetric I-V_b curves and have just shown the positive voltages in the resultant figures.

The self-consistently calculated I–V_b curves were shown in figure 4. The range of V_b is chosen from 0.0 to 2.0 V. For small V_b, i.e., the so-called Ohmic (linear) region, the current for pure graphene nanoribbon is the highest meanwhile that of the silicon-doped structure is higher than Germanium doped structure.

For the pure graphene nanoribbon, the current saturates at about 0.37μA. Thus, the device shows significant constant current at about 0.4 V.

For Silicon-doped structure the current decreases by increasing the bias voltage beyond the linear region (from 0.4V to 0.8V). This decrease continues until it reaches a constant amount of about zero. On the other word, the system reveals a negative differential resistance (NDR) behavior for about V_b=0.4 V to 0.8 V. For Germanium doped structure the current curve exhibits two hills and so two NDR behavior for two voltage intervals between V_b=0.4V to V_b=0.6 V as well as the interval between V_b=1V to V_b=1.2 V. A point worth of notice obtained from the diagram is that after the first NDR region, it takes a rather large voltage interval for the current to reach the second NDR region. This property may be crucial in the modern nanoelectronics switching devices. In conclusion, a multi switching behavior was observed for Germanium doped structure.

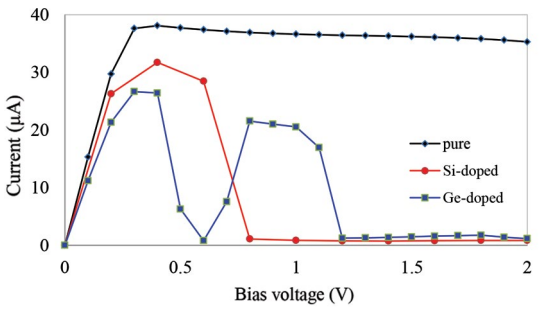

Fig. 4: I–V curves of pure, Si-doped and Ge-doped 2-zGNR at zero gate voltage.

I–V characteristics under different gate voltages

In order to undertake the gate effect on the transmission properties, the I-V_b for each system separately under different gate voltages (V_g) have been calculated. The resulting diagrams have been shown in figures 5a-c in which V_g is set to three different values (-3.0, 0.0 and 3.0 V) and V_b is in the range from 0.0 to 2.0 V in 0.1 V steps.

It is obvious from the figures that while the effect of the gate voltages to the I-V_b curves in pure graphene structure is not significant. For Si-doped structure, besides the similarity of I-V_b curves between the three applied V_g, a considerable difference in the current amount is observed. In the Ge-doped structure, instead of Si-doped case, we observe a dramatic change of the I-V_b characteristic for different gate voltages. As is seen from figure 5c, at V_g=0.0 V two picks in the current profile is present that suggests two NDR voltage range. The profile takes just one peak with a single NDR region for both of V_g=±3 V. It is considerable in the case of Si-doped and Ge-doped structures that suggest a gate–voltage-controllable device.

To explain these behaviors, the NDR regions have discussed by transmission spectrums for correspond bias voltages in the next part. Also, the partial atomic charge distributions of the channel region as a function of bias voltage have been discussed in the next section.

I-V characteristics and Transmission properties

By using the transmission formula, the current was determined by the integration of over electron energy in the bias window.

For the Ge-doped graphene, because of its two NDRs at the V_g=0.0 V, the transmission spectrum and the bias windows along with the integration areas at the important bias points have been presented in Figure 6. The considered bias values, corresponding to the maxima and minima points in the I-V_b curves, were related to the values of 26.663 (peak), 0.804 (valley), 21.542 (peak) and 1.158 μA (valley). This figure, nevertheless, showed that when the bias voltage was increased from 0.4 to 0.6 and 0.8 to 1.2 V, area under the transmission curve was decreased; on the other hand from 0.0 to 0.4 and 0.6 to 0.8 V, this area was increased. In other NDR regions the same analyses were done, but for brevity, they have not been presented here.

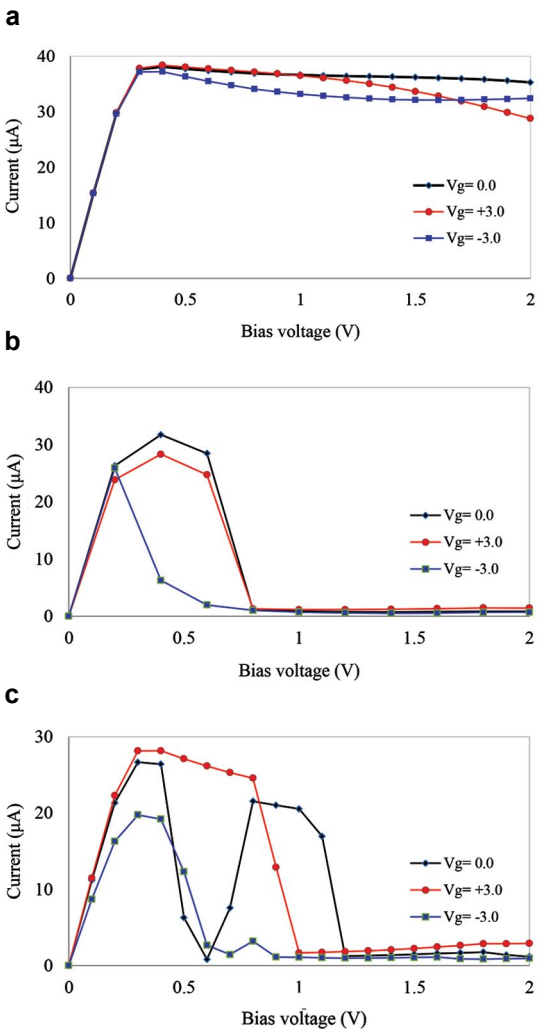

Fig. 5: I–V curves for a) pure, b) Si-doped, and c) Ge-doped 2-zGNR at three studied gate voltages (+3.0, 0.0 and -3.0 volt).

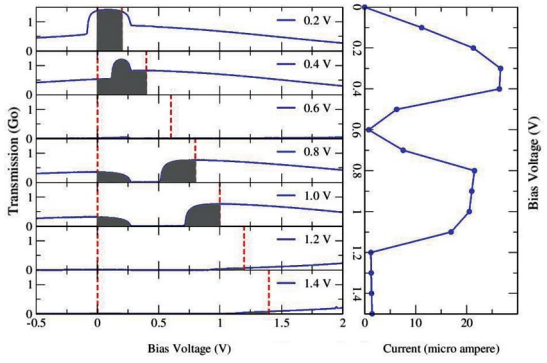

Fig. 6: Integrated bias windows of transmission spectrums at corresponding bias voltages to the maxima and minima points in the I-V_b curve for Ge-doped at V_g=0.0 V.

The partial atomic charge distribution

Pure 2-ZGNR system

Changing of the partial atomic charge in the scattering region between the two electrodes, as well, explained the I-V_b characteristics. For this idea the partial atomic charge distribution in the center part of the system's scattering region containing those carbon atoms at the left (CL) and right (CR) sides of substituted atoms which are connected to substituted atoms (CC) has been investigated for different bias voltages.

By Mulliken population analysis, the variations of the partial atomic charge distribution (at CL, CR and CC) by increasing the bias voltage (from 0.0 to 2.0 V) at the imposed gate voltages (0.0, 3.0 and -3.0 V) have been studied. The results have been shown for pure, Si-doped and Ge-doped 2-zGNR as figures 7, 8 and 9, respectively.

For pure graphene nanoribbon while the partial atomic charge on CC atom doesn't have any change by the bias voltage, the partial atomic charge on CR carbon decreases with corresponding increases on CL. The curves are almost the same with just small shifts for the three gate voltages. On the other word, the diagrams show an increase of the partial atomic charge on the left side carbon with a commuting decrease on the right side carbon and it is constant on the central substituted atom. All the above results show that the movements of the electrons are from the left atom to the right atom via the central substituted atom. Due to the constant amount of partial atomic charge on the CC atom of this structure, we expect a direct relationship between the current and the difference of partial atomic charge on the CL and CR by applying the bias voltage. The diagrams of figure 5a justify this claim; the current increases from 0.0 to 0.4 volt, as is shown in figures 7a- c, being zero at un-biased condition, the difference of partial atomic charge on CL and CR increases by increasing the bias voltage. However, in both of the current and partial atomic charge diagrams, an abrupt change is observed at 0.4 V. The saturation of the current above 0.4 V can be ascribed to the constant charge capacity of the channel which does not let continues increase of its charge and is obvious from the constant amount of the channel charge by changing the bias voltage beyond 0.4 V. The interpretation of the corresponding diagrams at the next paragraph for the other two systems, Ge- and Si-doped, will clarify this point.

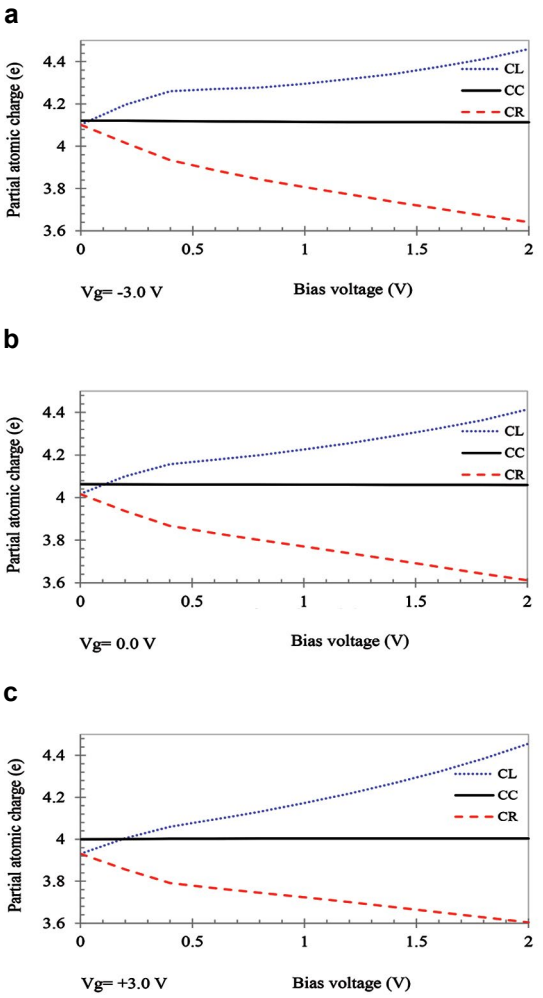

Fig. 7: Changing of partial atomic charges on the CL, CC, and CR atoms at different bias voltages and a) V_g=-3.0 b) V_g=0.0, c) V_g=+3.0 V for pure 2-zGNR.

Si-doped 2-ZGNR system

The partial atomic charge for Si-doped graphene nanoribbon at several bias voltages and three imposed gate voltages are plotted in figures 8a- c. As can be seen from these figures, at very small biases, it appears that the partial atomic charge on silicon is constant and is accompanied by increase of partial atomic charge on the left side carbon atom and decrease on the right side carbon atom. These results are in an increasing current by the applied voltage. Then a decrease of the partial atomic charge of silicon atom induces NDR in the current diagram. The more elevated voltages keep the silicon atom's partial atomic charge constant and results in saturation of the current, as in the pure GNR.

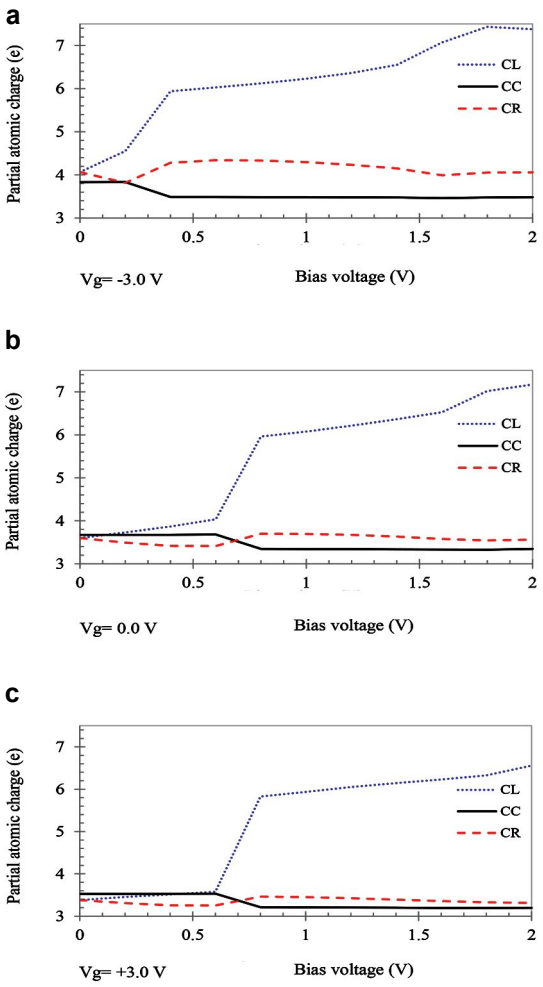

Fig. 8: Changing of partial atomic charges on the CL, CC, and CR atoms at different bias voltages and a) V_g=-3.0 b) V_g=0.0, c) V_g=+3.0 V for Si-doped 2-zGNR.

Ge-doped 2-ZGNR system

For Ge-doped graphene nanoribbon the partial atomic charge at several bias voltages and three imposed gate voltages are plotted in figures 9a- c. As can be seen from figure 9b at zero gate voltage the partial atomic charge on Ge is constant up to 0.6 V and then undergoes a decrease which is followed by an increase. It keeps a constant amount until another decrease. Looking back to figure 5c we observe a corresponding behavior in the current-voltage plot where two NDRs are observed just at the voltages of partial atomic charge decreasing.

The most important phenomenon achieved by these investigations are those first, the abrupt varying of the partial atomic charge of substituted atom is simultaneous with the changing the partial atomic charge on the left and right sides, carbon atoms, and the second is that there are almost the same extreme points for both of the substituted atom partial atomic charges and current curves.

In this system at other applied gate voltages as is observed from the figures 9b and 9c, the partial atomic charge on Ge undergoes a decrease after an interval of a constant amount of changing the bias voltage. Then it rests on this constant amount.

Comparing the diagrams with the corresponding current-voltage plot manifests, again, that the current follows changes of the partial atomic charge showing just one NDR voltage interval.

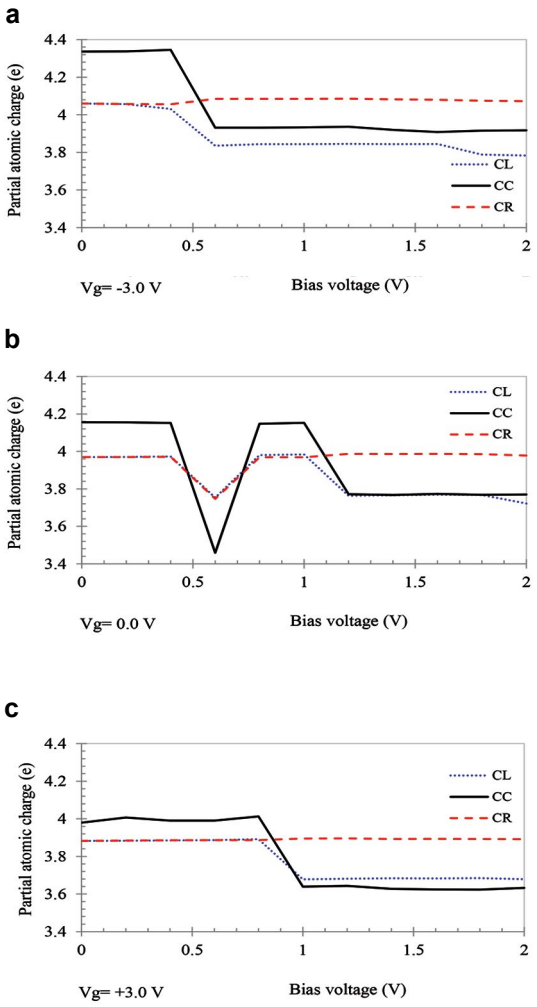

Fig. 9: Changing of partial atomic charges on the CL, CC, and CR atoms at different bias voltages and a) V_g=-3.0 b) V_g=0.0, c) V_g=+3.0 V for Ge-doped 2-zGNR.

CONCLUSION

In this work the quantum transport properties of pure and functionalized infinite lead-connection region-lead system based on zigzag graphene nanoribbon (2-zGNR) by applying the DFT+NEGF

first principles method have been investigated. The connection region between the two leads is chemically doped with Silicon and Germanium (the central two atoms). The main aims of this research were to computationally study the effect of the doping functionalization and variations of the gate voltages on the quantum transport of the 2-zGNR at different bias voltages. The results were presented as the current versus the bias voltage ($I\text{-}V_b$) curves with unique properties for per studied systems, showing one or multiple negative differential resistances (NDR). Therefore, a multi switching behavior of gate voltage 0.0 V, and nano-switch behavior at other studied gate voltages (V_g=±3.0 V) were observed for Germanium doped 2-zGNR. Also, the Silicon doped one could be used as nano-switch at studied gate voltages. Whereas, there weren't any switching behaviors for pure 2-zGNR. The multiple NDR's was discussed and interpreted in the terms of the transmission spectrum and its integral inside of the corresponding bias window. The partial atomic charge distribution in the center part of the system's scattering region containing carbon atoms at the left and right sides of substituted atoms which are connected to substituted atoms has been investigated for different bias voltages, too. The most important phenomenon achieved by these investigations are those first, the abrupt varying of the partial atomic charge of substituted atom is simultaneous with the changing the partial atomic charge on the left and right sides, carbon atoms, and the second is that there are almost the same extreme points for both of the substituted atoms partial atomic charge and current curves.

CONFLICT OF INTEREST

The authors declare that there is no conflict of interests regarding the publication of this manuscript.

REFERENCES

1. D. Gao, F. Scholz, H.-G. Nothofer, W.E. Ford, U. Scherf, J.M. Wessels, A. Yasuda, F. von Wrochem, Fabrication of Asymmetric Molecular Junctions by the Oriented Assembly of Dithiocarbamate Rectifiers, J. Am. Chem. Soc., 133, 5921 (2011).
2. J.B. Pan, Z.H. Zhang, K.H. Ding, X.Q. Deng, C. Guo, Current rectification induced by asymmetrical electrode materials in a molecular device, Appl. Phys. Lett., 98, 092102 (2011).
3. P. Parida, S.K. Pati, A. Painelli, Negative differential conductance in nanojunctions: A current constrained approach, Phys. Rev. B: Condens. Matter, 83, 165404 (2011).
4. Q. Liu, G. Luo, R. Qin, H. Li, X. Yan, C. Xu, L. Lai, J. Zhou, S. Hou, E. Wang, Z. Gao, J. Lu, Negative differential resistance in parallel single-walled carbon nanotube contacts, Phys. Rev. B: Condens. Matter, 83, 155442 (2011).
5. E.S. Tam, J.J. Parks, W.W. Shum, Y.-W. Zhong, M.E.B. Santiago-Berríos, X. Zheng, W. Yang, G.K.L. Chan, H.D. Abruña, D.C. Ralph, Single-Molecule Conductance of Pyridine-Terminated Dithienylethene Switch Molecules, ACS Nano, 5, 5115 (2011).
6. M.K. Ashraf, N.A. Bruque, J.L. Tan, G.J.O. Beran, R.K. Lake, Conductance switching in diarylethenes bridging carbon nanotubes, The Journal of Chemical Physics, 134, 024524 (2011).
7. Y. Xue, M.A. Ratner, End group effect on electrical transport through individual molecules: A microscopic study, Phys. Rev. B: Condens. Matter, 69, 085403 (2004).
8. M. Qiu, Z.H. Zhang, X.Q. Deng, J.B. Pan, End-group effects on negative differential resistance and rectifying performance of a polyyne-based molecular wire, Appl. Phys. Lett., 97, 242109 (2010).
9. Y. Ma, A.S. Foster, A.V. Krasheninnikov, R.M. Nieminen, Nitrogen in graphite and carbon nanotubes: Magnetism and mobility, Phys. Rev. B: Condens. Matter, 72, 205416 (2005).
10. J. Zheng, X. Yan, L. Yu, H. Li, R. Qin, G. Luo, Z. Gao, D. Yu, J. Lu, Family-Dependent Rectification Characteristics in Ultra-Short Graphene Nanoribbon p–n Junctions, The J. Phys. Chem. C, 115, 8547 (2011).
11. V.M. García-Suárez, C.J. Lambert, Non-trivial length dependence of the conductance and negative differential resistance in atomic molecular wires, Nanotechnology, 19, 455203 (2008).
12. L. Senapati, R. Pati, M. Mailman, S.K. Nayak, First-principles investigation of spin-polarized conductance in atomic carbon wires, Phys. Rev. B: Condens. Matter, 72, 064416 (2005).
13. Y. He, C. Zhang, C. Cao, H.-P. Cheng, Effects of strain and defects on the electron conductance of metallic carbon nanotubes, Phys. Rev. B: Condens. Matter, 75, 235429 (2007).
14. I. Romanovsky, C. Yannouleas, U. Landman, Edge states in graphene quantum dots: Fractional quantum Hall effect analogies and differences at zero magnetic field, Phys. Rev. B: Condens. Matter, 79, 075311 (2009).
15. O. Chiatti, J.T. Nicholls, Y.Y. Proskuryakov, N. Lumpkin, I. Farrer, D.A. Ritchie, Quantum Thermal Conductance of Electrons in a One-Dimensional Wire, Phys. Rev. Lett., 97, 056601 (2006).
16. M. Qiu, K.M. Liew, Position effects of single vacancy on transport properties of single layer armchair h-BNC heterostructure, Physical Chemistry Chemical Physics, 14, 11478 (2012).
17. W.Y. Kim, Y.C. Choi, S.K. Min, Y. Cho, K.S. Kim, Application of quantum chemistry to nanotechnology: electron and spin transport in molecular devices, Chem. Soc. Rev., 38, 2319 (2009).
18. Y. Xu, G. Zhang, B. Li, Large Negative Differential Resistance in a Molecular Junction of Carbon Nanotube and Anthracene, The Journal of Physical Chemistry B, 112, 16891 (2008).
19. K.H. Khoo, J.B. Neaton, Y.W. Son, M.L. Cohen, S.G. Louie, Negative Differential Resistance in Carbon Atomic Wire-Carbon Nanotube Junctions, Nano Letters, 8, 2900 (2008).
20. W.Y. Kim, S.K. Kwon, K.S. Kim, Negative differential resistance of carbon nanotube electrodes with asymmetric coupling phenomena, Phys. Rev. B: Condens. Matter, 76, 033415 (2007).
21. A. Iyengar, T. Luo, H.A. Fertig, L. Brey, Conductance through graphene bends and polygons, Phys. Rev. B: Condens. Matter, 78, 235411 (2008).
22. S.U. Lee, M. Khazaei, F. Pichierri, Y. Kawazoe, Electron transport through carbon nanotube intramolecular heterojunctions with peptide linkages, Physical Chemistry Chemical Physics, 10, 5225 (2008).
23. P.C.P. Watts, W.K. Hsu, D.P. Randall, H.W. Kroto, D.R.M. Walton, Non-linear current-voltage characteristics of electrically conducting carbon nanotube-polystyrene composites, Physical Chemistry Chemical Physics, 4, 5655 (2002).
24. L.A. Agapito, E.J. Bautista, J.M. Seminario, Conductance model

of gold-molecule-silicon and carbon nanotube-molecule-silicon junctions, Phys. Rev. B: Condens. Matter, 76, 115316 (2007).

25. J. Taylor, H. Guo, J. Wang, Phys. Rev. B, 63, 245407 (2001).
26. Y.-P. An, C.-L. Yang, M.-S. Wang, X.-G. Ma, D.-H. Wang, First-Principles Study of Electronic Transport Properties of Dodecahedrane C20H20 and Its Endohedral Complex Li@C20H20, The J. Phys. Chem. C, 113, 15756 (2009).
27. W. Haiss, S. Martin, L.E. Scullion, L.
28. A. Iyengar, T. Luo, H.A. Fertig, L. Brey, Conductance through graphene bends and polygons, Phys. Rev. B: Condens. Matter, 78 (2008) 235411.
29. S.U. Lee, M. Khazaei, F. Pichierri, Y. Kawazoe, Electron transport through carbon nanotube intramolecular heterojunctions with peptide linkages, Physical Chemistry Chemical Physics, 10 (2008) 5225-5231.
30. P.C.P. Watts, W.K. Hsu, D.P. Randall, H.W. Kroto, D.R.M. Walton, Non-linear current-voltage characteristics of electrically conducting carbon nanotube-polystyrene composites, Physical Chemistry Chemical Physics, 4 (2002) 5655-5662.
31. L.A. Agapito, E.J. Bautista, J.M. Seminario, Conductance model of gold-molecule-silicon and carbon nanotube-molecule-silicon junctions, Phys. Rev. B: Condens. Matter, 76 (2007) 115316.
32. J. Taylor, H. Guo, J. Wang, Phys. Rev. B, 63 (2001) 245407.
33. Y.-P. An, C.-L. Yang, M.-S. Wang, X.-G. Ma, D.-H. Wang, First-Principles Study of Electronic Transport Properties of Dodecahedrane C20H20 and Its Endohedral Complex Li@C20H20, The J. Phys. Chem. C, 113 (2009) 15756-15760.
34. W. Haiss, S. Martin, L.E. Scullion, L. Bouffier, S.J. Higgins, R.J. Nichols, Anomalous length and voltage dependence of single molecule conductance, Physical Chemistry Chemical Physics, 11 (2009) 10831-10838.
35. C.-K. Wang, Y. Fu, Y. Luo, A quantum chemistry approach for current-voltage characterization of molecular junctions, Physical Chemistry Chemical Physics, 3 (2001) 5017-5023.
36. A.K. Geim, K.S. Novoselov, The rise of graphene, Nat Mater, 6 (2007) 183-191.
37. Z. Chen, Y.-M. Lin, M.J. Rooks, P. Avouris, Graphene nano-ribbon electronics, Physica E: Low-dimensional Systems and Nanostructures, 40 (2007) 228-232.
38. M.Y. Han, Ouml, B. zyilmaz, Y. Zhang, P. Kim, Phys. Rev. Lett., 98 (2007) 206805.
39. M.I. Katsnelson, K.S. Novoselov, A.K. Geim, Chiral tunnelling and the Klein paradox in graphene, Nat Phys, 2 (2006) 620-625.
40. Y.-M. Lin, K.A. Jenkins, A. Valdes-Garcia, J.P. Small, D.B. Farmer, P. Avouris, Operation of Graphene Transistors at Gigahertz Frequencies, Nano Letters, 9 (2008) 422-426.
41. X. Feng, N. Chandrasekhar, H. Su, K. Müllen, Ballistic Electron Microscopy of Nanographene Layers, Nano Letters, 8 (2008) 4259-4264.
42. D. Abdula, T. Ozel, K. Kang, D.G. Cahill, M. Shim, Environment-Induced Effects on the Temperature Dependence of Raman Spectra of Single-Layer Graphene, The J. Phys. Chem. C, 112 (2008) 20131-20134.
43. M. Wang, C.M. Li, Negative differential resistance in oxidized zigzag graphene nanoribbons, Physical Chemistry Chemical Physics, 13 (2011) 1413-1418.
44. M. Wu, X. Wu, X.C. Zeng, Exploration of Half Metallicity in Edge-Modified Graphene Nanoribbons, The J. Phys. Chem. C, 114 (2010) 3937-3944.
45. Z. Li, J. Yang, J.G. Hou, Half-Metallicity in Edge-Modified Zigzag Graphene Nanoribbons, J. Am. Chem. Soc., 130 (2008) 4224-4225.
46. H. Kim, K. Lee, S.I. Woo, Y. Jung, On the mechanism of enhanced oxygen reduction reaction in nitrogen-doped graphene nanoribbons, Physical Chemistry Chemical Physics, 13 (2011) 17505-17510.
47. J. Zeng, K.-Q. Chen, J. He, Z.-Q. Fan, X.-J. Zhang, Nitrogen doping-induced rectifying behavior with large rectifying ratio in graphene nanoribbons device, J. Appl. Phys., 109 (2011) -.
48. S. Dutta, S.K. Pati, Half-Metallicity in Undoped and Boron Doped Graphene Nanoribbons in the Presence of Semilocal Exchange-Correlation Interactions, The Journal of Physical Chemistry B, 112 (2008) 1333-1335.
49. J. Li, Z. Li, G. Zhou, Z. Liu, J. Wu, B.-L. Gu, J. Ihm, W. Duan, Spontaneous edge-defect formation and defect-induced conductance suppression in graphene nanoribbons, Phys. Rev. B: Condens. Matter, 82 (2010) 115410.
50. S. Dutta, S.K. Pati, Edge reconstructions induce magnetic and metallic behavior in zigzag graphene nanoribbons, Carbon, 48 (2010) 4409-4413.
51. S. Dutta, A.K. Manna, S.K. Pati, Intrinsic Half-Metallicity in Modified Graphene Nanoribbons, Phys. Rev. Lett., 102 (2009) 096601.
52. J. He, K.-Q. Chen, Z.-Q. Fan, L.-M. Tang, W.P. Hu, Transition from insulator to metal induced by hybridized connection of graphene and boron nitride nanoribbons, Appl. Phys. Lett., 97 (2010) 193305.
53. E.A. Basheer, P. Parida, S.K. Pati, Electronic and magnetic properties of BNC nanoribbons: a detailed computational study, New Journal of Physics, 13 (2011) 053008.
54. B. Akdim, R. Pachter, Switching Behavior of Carbon Chains Bridging Graphene Nanoribbons: Effects of Uniaxial Strain, ACS Nano, 5 (2011) 1769-1774.
55. E. Erdogan, I. Popov, G. Seifert, Robust electronic and transport properties of graphene break nanojunctions, Phys. Rev. B: Condens. Matter, 83 (2011) 245417.
56. V.A. Rigo, R.H. Miwa, A.J.R. da Silva, A. Fazzio, Mn dimers on graphene nanoribbons: An ab initio study, J. Appl. Phys., 109 (2011) 053715.
57. Z. Zhang, B. Liu, K.-C. Hwang, H. Gao, Surface-adsorption-induced bending behaviors of graphene nanoribbons, Appl. Phys. Lett., 98 (2011) 121909.
58. N. Kharche, Y. Zhou, K.P. O'Brien, S. Kar, S.K. Nayak, Effect of Layer Stacking on the Electronic Structure of Graphene Nanoribbons, ACS Nano, 5 (2011) 6096-6101.
59. J. Zeng, K.-Q. Chen, J. He, X.-J. Zhang, W.P. Hu, Rectifying and successive switch behaviors induced by weak intermolecular interaction, Organic Electronics, 12 (2011) 1606-1611.
60. J. Zeng, K.-Q. Chen, C.Q. Sun, Electronic structures and transport properties of fluorinated boron nitride nanoribbons, Physical Chemistry Chemical Physics, 14 (2012) 8032-8037.
61. The code, OPENMX, pseudoatomic basis functions, and pseudopotentials are available on a web site 'http://www.openmxsquare.org'.
62. J.P. Perdew, K. Burke, M. Ernzerhof, Generalized Gradient Approximation Made Simple, Phys. Rev. Lett., 77 (1996) 3865-3868.
63. N. Troullier, J.L. Martins, Efficient pseudopotentials for plane-wave calculations, Phys. Rev. B: Condens. Matter, 43 (1991) 1993-2006.
64. T. Ozaki, Variationally optimized atomic orbitals for large-scale electronic structures, Phys. Rev. B: Condens. Matter, 67 (2003) 155108.
65. T. Ozaki, H. Kino, Numerical atomic basis orbitals from H to Kr, Phys. Rev. B: Condens. Matter, 69 (2004) 195113.